Four-cluster chimera state in non-locally coupled phase oscillator systems with an external potential*

Zhu Yun(朱 云)[a)b)], Zheng Zhi-Gang(郑志刚)[a)†], and Yang Jun-Zhong(杨俊忠)[c)]

[a)] *Department of Physics, Beijing Normal University, Beijing* 100875, *China*
[b)] *School of Science, Jiangxi University of Science and Technology, Ganzhou* 341000, *China*
[c)] *School of Science, Beijing University of Posts and Telecommunications, Beijing* 100876, *China*

(Received 25 February 2013; revised manuscript received 29 March 2013)

Dynamics of a one-dimensional array of non-locally coupled Kuramoto phase oscillators with an external potential is studied. A four-cluster chimera state is observed for the moderate strength of the external potential. Different from the clustered chimera states studied before, the instantaneous frequencies of the oscillators in a synchronized cluster are different in the presence of the external potential. As the strength of the external potential increases, a bifurcation from the two-cluster chimera state to the four-cluster chimera states can be found. These phenomena are well predicted analytically with the help of the Ott–Antonsen ansatz.

Keywords: chimera state, non-local coupling, Kuramoto oscillators and Ott–Antonsen ansatz

PACS: 05.45.Xt **DOI:** 10.1088/1674-1056/22/10/100505

1. Introduction

Chimera state is a type of spatiotemporal pattern in which some of the identical oscillators are coherent and synchronous while others remain incoherent.[1–5] They usually appear in systems with non-local couplings and could only be built for proper initial conditions.[6] Chimera state was first numerically observed by Kuramoto and his colleagues[1,2] in simulations of the non-locally coupled complex Ginzburg–Landau equations. For two-dimensional (2D) arrays of non-locally coupled oscillators, a spiral wave chimera state[7,8] was discovered. Abrams and Strogatz[3] found an exact solution for this state in a ring of phase oscillators with a cosine-kernel coupling. Furthermore, the clustered chimera state,[9,10] which has spatially distributed phase coherence separated by incoherence with adjacent coherent regions in antiphase, was found in the studies of the non-locally coupled oscillators with a time delay. Zhu *et al.*[11] found a two-cluster chimera state without time-delayed coupling. Besides, Abrams *et al.*[12] found a breathing chimera state in a model consisting of two interacting sub-populations of oscillators. Pikovsky and Rosenblum[13] considered oscillator ensembles consisting of several sub-populations of identical units, with a general heterogeneous coupling between sub-populations, through which they acquired a quasiperiodic chimera state. Laing[14,15] summarized chimera states in several heterogeneous networks of coupled phase oscillators and analyzed the state by applying the Ott–Antonsen ansatz[16] to one-dimensional (1D) and 2D systems. He pointed out that a breathing chimera state exists in 1D systems when the parameter heterogeneity is introduced.

Chimera states can be self-organized in many systems that are inevitably impacted by the external environment. Specifically, it is significant to study the chimera dynamics when the system is put in an external potential. Ma *et al.*[17] studied the system consisting of sub-populations of oscillators with an external potential and found the alternating chimera state. Chimera states can be found even in the simplest systems such as the 1D array of uniform oscillators. It is thus necessary to study the behaviors of such simple systems in the presence of external potential. In this work, we study a 1D array of non-locally coupled identical phase oscillators with an external potential. We find that for a moderate strength of the potential, a four-cluster chimera state can emerge under the modulation of this external potential. Furthermore, the instantaneous frequencies of the four clusters are found to be different from those of the clustered chimera state observed previously in Refs. [9]–[11]. The emergence of the four-cluster chimera state in this model is analyzed by the Ott–Antonsen ansatz, which agrees well with our numerical results. The presence of multiple-cluster chimera states may shed some light on the studies of issues such as the unihemispheric sleeping[18,19] and the ability to handle the multiple task in neurology.[20]

2. Model

The dynamics of a 1D array of non-locally coupled identical phase oscillators with a periodic potential $V(\theta) = A_0 \cos\theta$

*Project supported by the National Natural Science Foundation of China (Grant Nos. 10875011 and 11075016), the 973 Project (Grant No. 2007CB814805), the Fundamental Research Funds for the Central Universities, the Foundation for Doctoral Training from the Ministry of Education of China.

†Corresponding author. E-mail: zgzheng@bnu.edu.cn

© 2013 Chinese Physical Society and IOP Publishing Ltd

can be described as

$$\frac{\partial}{\partial t}\theta(x,t) = \omega + A_0 \sin\theta - \int_{-\pi}^{\pi} G(x-x') \times \sin[\theta(x,t) - \theta(x',t) + \alpha]\,\mathrm{d}x'. \quad (1)$$

Here, $\theta(x,t)$ represents the phase of the oscillator at position x at time t. The variable x is limited in the range $[-\pi,\pi]$, and the periodic boundary condition is imposed in this paper. A_0 describes the strength of the external potential. The natural frequency ω (the same for all oscillators) is set to be $\omega = 0$ for convenience. It should be noted that a non-zero natural frequency cannot be eliminated and will affect the chimera dynamics in the presence of an overall pinning potential ($A_0 \neq 0$). This is another issue, which will be discussed elsewhere. The angle α ($0 \leq \alpha \leq \pi/2$) is a tunable parameter that describes the phase shift between oscillators at x and x' (also called the frustration). The kernel function $G(x-x')$ provides the nonlocal coupling between the oscillator located at x and that at x'. $G(x)$ is an even, non-negative function and decreases with $|x|$ increasing along the array. $\int_{-\pi}^{\pi} G(x)\,\mathrm{d}x = 1$. For simplicity, $G(x)$ is of the cosine form:

$$G(x) = \frac{1}{2\pi}(1 + A\cos x). \quad (2)$$

The key idea behind the analysis of the chimera state is the introduction of a mean-field-like quantity, namely, a complex order parameter $R\mathrm{e}^{\mathrm{i}\Theta}$,[1–3] which is defined as

$$R(x,t)\,\mathrm{e}^{\mathrm{i}\Theta(x,t)} = \int_{-\pi}^{\pi} G(x-x')\,\mathrm{e}^{\mathrm{i}\theta(x',t)}\,\mathrm{d}x'. \quad (3)$$

Then equation (1) becomes

$$\frac{\partial\theta}{\partial t} = \omega + A_0 \sin\theta - R\sin(\theta - \Theta + \alpha). \quad (4)$$

When there is no external potential, i.e., $A_0 = 0$, it has been revealed that the system has three collective dynamical states: the synchronized state, the single chimera state,[1,3] and the two-cluster chimera state.[11] The two-cluster chimera state has two synchronized clusters with a phase difference around π. The complex order parameter (3) is temporally oscillating due to the finite size effect.[11] When the amplitude of the external potential A_0 is large enough (for example, $A_0 > 1$), the system will approach the synchronized state, and $R = 1$. In this case, the system steps into the equilibrium state $\sin\theta(x) = 1/A_0$.

It is interesting to explore the influence of an external field for moderate amplitude of A_0. In this case, the competition between the external potential and the spatial coupling may lead to more complicated and significant dynamics of the system.

3. Simulation and results

Generally, the emergence of chimera state depends on the choice of the initial condition. The system usually evolves to completely synchronized states for random initial distributions of phases. If one starts from the initial condition that there is a gap π between the phases of two segments, the system will evolve into the four-cluster chimera state. Specifically, we can take the initial conditions as follows:

$$\theta(x,0) = \begin{cases} 2\pi(r+0.25)\,\mathrm{e}^{-3x^2}, & x \leq 0, \\ 2\pi(r-0.25)\,\mathrm{e}^{-3x^2}, & x > 0, \end{cases} \quad (5)$$

where r is a uniform random number among [0, 1].

In Fig. 1, the results are shown for parameters $\beta = \pi/2 - \alpha = 0.10$, $A = 0.995$, and $A_0 = 0.4$. Figure 1(a) shows a snapshot of four-cluster chimera state. One can observe that the system has four inherent clusters in which the oscillators are synchronized. Between these clusters, the oscillators are de-synchronized and their phases are randomly distributed in $[-\pi,\pi]$.

The averaged angular velocity $\langle\dot{\theta}(x)\rangle$ and the fluctuations of the instantaneous angular velocity

$$\sigma = \sqrt{\langle(\dot{\theta}(x) - \langle\dot{\theta}(x)\rangle)^2\rangle}$$

are introduced to characterize the chimera state, where $\langle\cdot\rangle$ is the average value in a time interval of 1000 units. Figure 1(b) shows the spatial profile of $\langle\dot{\theta}(x)\rangle$ and σ^2. Clearly, there are four coherent clusters, inside which the averaged frequencies of the oscillators are the same. Different from the clustered chimera state studied in Refs. [9]–[11], the frequencies of the oscillators in different clusters are not all the same. According to the averaged frequency, four clusters could be divided into two groups. Each group contains two clusters with the same average frequency. In one group named the 'dynamical group', the frequency of oscillators is around -0.35. In another group called the 'static group', the frequency of oscillators is 0. The inherent clusters in the same group are separated by the clusters in another group. According to the distribution of fluctuation σ^2, it can be found that σ is small in the synchronized clusters and is large in the unsynchronized region. In addition, σ is inhomogeneous in the cluster of the dynamical group (denoted as the D-cluster) and inhomogeneous in the cluster of the static group (denoted as S-cluster). But the values of σ of all oscillators are larger than zero, which means that the instantaneous angular velocity is time-dependent even in the synchronized cluster.

To obtain a deeper understanding, we plot the time evolution of the instantaneous angular velocity $\dot{\theta}(x,t)$ in Fig. 1(d). It can be seen that the oscillators in the same D-cluster have the same instantaneous angular velocity though the velocity varies periodically. Meanwhile the oscillators in different D-clusters have different instantaneous angular velocities and there is a half period time delay. Because σ is inhomogeneous, the oscillators have different instantaneous angular velocities in

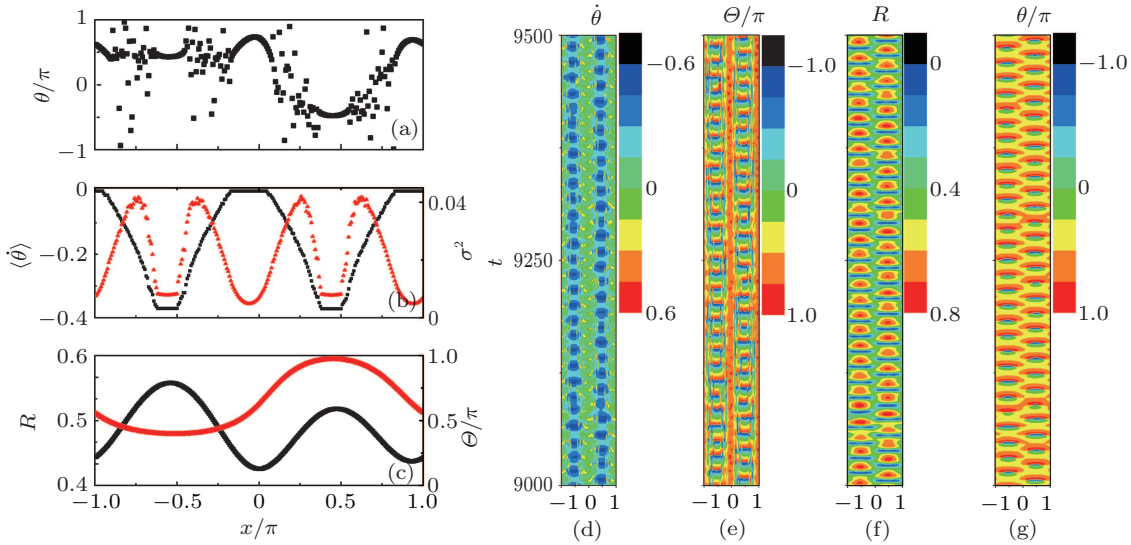


Fig. 1. (color online) (a) A snapshot of the phase pattern for the four-cluster chimera state when the steady state is reached. Equation (1) is integrated by using the Runge–Kutta method with fixed time step d$t = 0.1$. The oscillator number $N = 256$, $\beta = 0.10$, and $A = 0.995$. (b) The distribution of $\langle\dot{\theta}(x)\rangle$ of individual oscillators averaged over 1000 time units (square/black) and fluctuations of the instantaneous angular velocity σ^2 (triangle/red). (c) A snapshot of the amplitude $R(x)$ (square/black) and $\Theta(x)$ (triangle/red) of complex order parameter. (d)–(g) The time evolutions of $\dot{\theta}(x)$, $R(x)$, $\Theta(x)/\pi$, and $\theta(x)/\pi$, respectively. The horizontal axis represents the position x, and the vertical axis denotes the time t.

the same S-cluster. From Fig. 1(d), the angular velocity of these oscillators is around 0 and varies periodically, and the phase of the oscillators in the S-cluster is located in the range $[\pi, 3\pi/2]$ as shown in Fig. 1(e).

Now, we further study the complex order parameter. The snapshot of $R(x)$ and $\Theta(x)$ depicted in Fig. 1(c) shows that the distribution of R has two maxima and two minima. It is very interesting that the maxima and minima correspond to the D-cluster and the S-cluster respectively. In previous studies of chimera state, the synchronized clusters are located at the positions around the peaks of the complex order parameter R. Why are the oscillators of the S-cluster located at the minima?

In order to answer this question, we plot the spatiotemporal evolutions of $R(x,t)$ and $\Theta(x,t)$ in Figs. 1(f) and 1(g). It can be found that the values of R for S-clusters are around $A_0(= 0.40)$ and the values of Θ are in the range around $\pi/2$. The last two terms on the right-hand side of Eq. (4) balance each other, thus the frequency of oscillators in the clusters is around 0. When ω is apart from 0, the last two terms on the right-hand side of Eq. (4) are not counterbalanced. Then the four-cluster chimera state cannot exist any longer. In the region of D-cluster, it can be found that the complex order parameter is oscillatory. When R reaches its minimum in one cluster, R in the other one reaches its maximum. Furthermore, the evolution of R of the D-cluster has the same period as that of the oscillator in the cluster and the values of R for different D-clusters have the same pattern but with a time delay.

The oscillation of R in the two-cluster chimera state is caused by the finite size effect.[11] Is the oscillation of R in the four-cluster chimera state caused by the same reason? We study the R_d that varies with time at different sizes of the system in Fig. 2, in which R_d is the amplitude of complex order parameter of the central oscillator inside one D-cluster. It is shown that R_d is oscillating at different sizes of system in Fig. 2(a)–2(c). To characterize the oscillatory behavior, $\langle R_d\rangle$ (the time average of R_d) and $\sigma_R = \sqrt{\langle(R_d - \langle R_d\rangle)^2\rangle}$ (the fluctuations of R_d) are computed. The results of Fig. 2(d) show that $\langle R_d\rangle$ and σ_R are almost independent of system size,

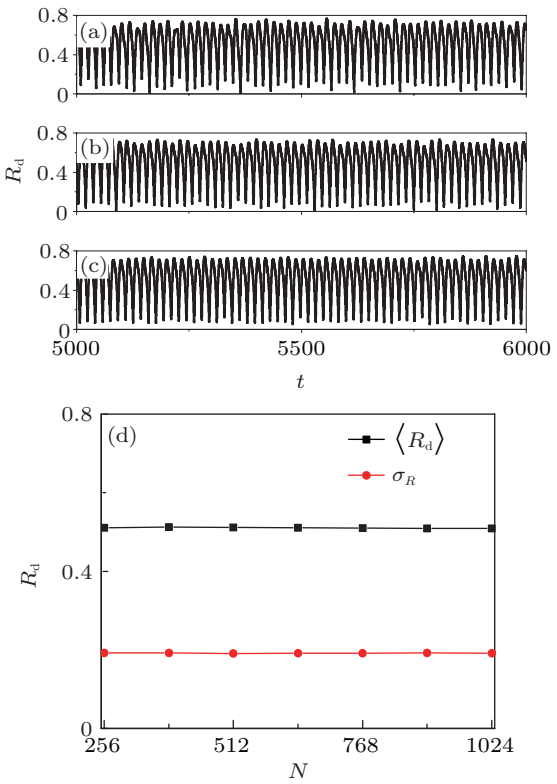


Fig. 2. (color online) The evolution of the amplitude of the complex order R_d of the oscillator in the center of one D-cluster. Panels (a), (b), and (c) are plotted for $N = 256$, 512, and 1024, respectively. Here $A_0 = 0.4$, $\beta = 0.10$, and $A = 0.995$. Panel (d) shows that $\langle R_d\rangle$ and σ_d vary with the system size.

indicating that the oscillating of R is unaffected by the system size.

Now we come to study the oscillation dynamic behaviors of $R(x,t)$ for different values of A_0. It is necessary to plot the evolutions of $R_{\max}(x)$ (the maximum of R) and $R_{\min}(x)$ (the minimum of R) of each oscillator in Figs. 3(a) and 3(b). It can be seen that $R_{\max}$ and $R_{\min}$ are large in the region of D-cluster with small A_0. For a moderate A_0, $R_{\max}$ is large in the region of D-cluster, but $R_{\min}$ is large in the region of S-cluster. Hence R is restricted in the range of A_0 in the S-cluster. The larger the value of A_0, the larger the range of the S-cluster is. When A_0 is large enough ($A_0 > 0.65$), oscillators in the system are synchronized and $R(x) = 1$, which is not shown in Fig. 3. Moreover, the position of D-clusters is fixed when A_0 is fixed as shown in Fig. 1(e), but it will change when the parameter A_0 is increased. We plot the relation between R_s and A_0 in Fig. 3(c), where R_s represents $R_{\min}$ of the central oscillator of one S-cluster (because the S-clusters do not exist while $A_0 < A_{0c}$, the central oscillator of one S-cluster is replaced by the central oscillator between two D-clusters) at different system sizes. It can be found that R_s does not crucially depend on system size. An interesting transition happens at a critical amplitude A_{0c}, where $R_s = 0$ when $A_0 < A_{0c} = 0.13$ and R_s obeys a typical scaling $R_s \propto (A_0 - A_{0c})^{1/2}$ while $A_0 > A_{0c}$. $R_s = 0$ corresponds to the two-cluster chimera states, and $R_s > 0$ represents the four-cluster chimera state. This transition implies that a Hopf bifurcation from the two-cluster chimera state to the four-cluster chimera state happens when increasing the amplitude of the external potential A_0.

Because the instantaneous angular velocities of the oscillators in different D-clusters with the external potential are not the same, the phase difference between two D-clusters does not fix at the antiphase value $\Delta\theta = \pi$. It is thus interesting to study the statistical behavior of the phase difference $\Delta\theta$ between the central oscillators of the two D-clusters. Figure 4(a) depicts the probability distribution of $\Delta\theta$ for a small $A_0 = 0.1$. It can be seen that there is a peak at $\Delta\theta = \pi$. This means that the frequency difference between the oscillators of D-clusters is so small that the phase difference can be fixed at the value π. This conforms to the case of the cluster chimera state[9–11] in the absence of the external potential. As the height of the external potential A_0 increases, the instantaneous angular velocity difference between the different D-clusters increases so that $\Delta\theta$ does not keep the value π any more. In Fig. 4(b), the probability distribution of $\Delta\theta$ has two peaks, which are symmetric to $\Delta\theta = \pi$. When A_0 is large enough, the system enters into the synchronized state and the center of the distribution $\Delta\theta \approx 0$. The distribution of $\Delta\theta$ becomes the single-peak type again as shown in Fig. 4(c).

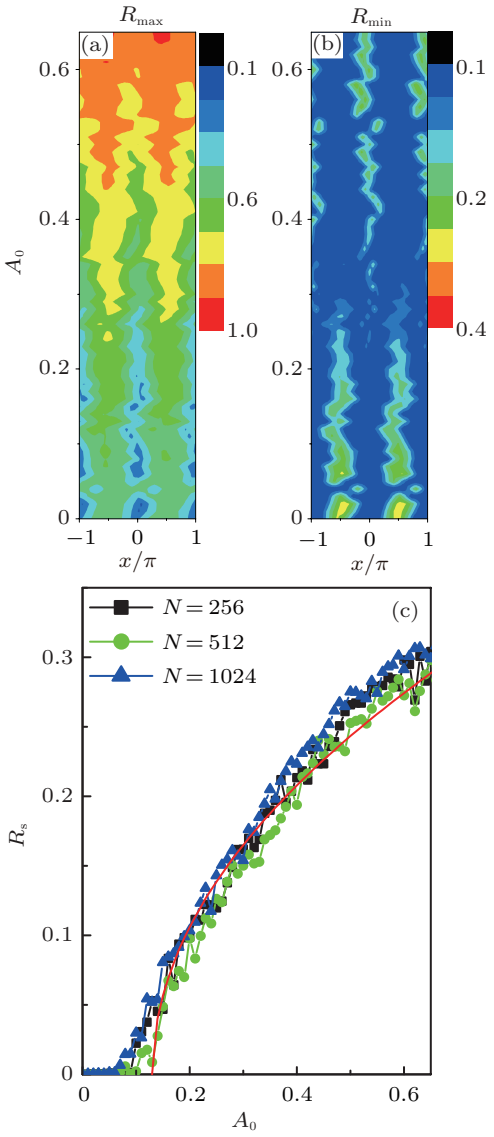


Fig. 3. (color online) (a) and (b): The contour graphs of the maximum $R_{\max}(x)$ and the minimum $R_{\min}(x)$ of $R(x,t)$ of the complex order parameter at different values of A_0; here $\beta = 0.10$, $A = 0.995$, and $N = 256$. Figure 3(c) shows the minima of amplitude of the complex order parameter of the oscillator in the center of one S-cluster R_s versus the potential strength A_0 at different system sizes $N = 256$ (black/square), $N = 512$ (green/circle), and $N = 1024$ (blue/triangle). The line is the fitting line obeying $0.4(A_0 - A_{0c})^{1/2}$, $A_{0c} = 0.13$.

The above statistical results indicate that the four-cluster chimera state discovered here is associated with the double-peak behavior of the distribution of the cluster phase difference. We further study how these peaks $\Delta\theta_m$ vary as A_0 is changed adiabatically from the initial condition given by Eq. (5), which is shown in Fig. 4(d). The adiabatic process can be easily implemented in simulations by adopting the final state for a value A_0 as the initial state for the next value $A_0 + \delta A_0$. Again one may clearly find a bifurcation at $A_0 = A_{0c}$, where the single peak of the phase-difference distribution becomes two peaks. It can be seen that the bifurcation is continuous in the process of the transition from the two-cluster chimera state to the four-cluster chimera state. When $A_0 > 0.65$, the system is synchronized and the peak is located

at $\Delta\theta = 0$. From Fig. 4(d), we can find that $\Delta\theta_{\rm m}$ drops off down to 0 at $A_0 = 0.65$. This is a discontinue transition from the four-cluster chimera state to the synchronous state.

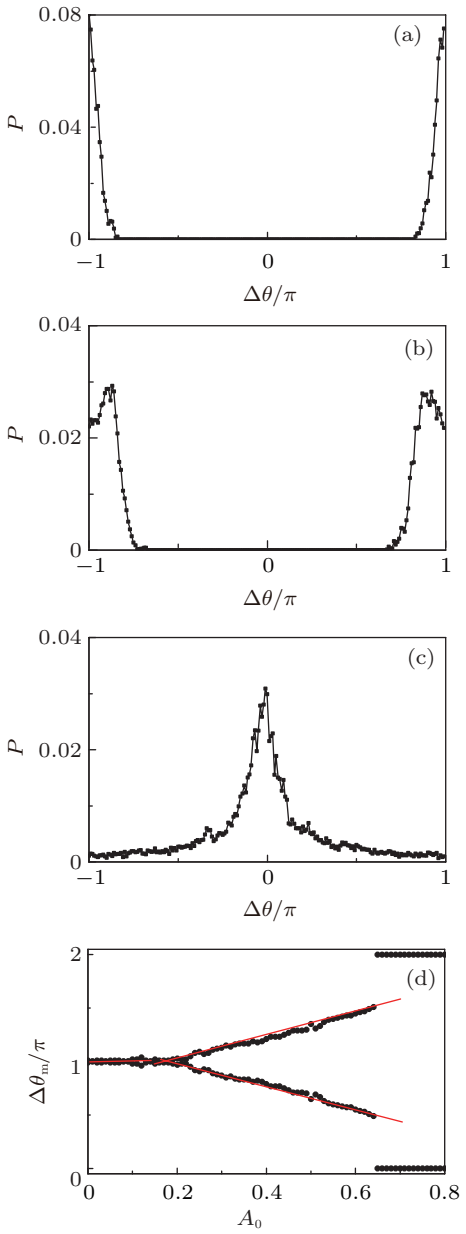


Fig. 4. (color online) The probability distribution of the phase difference $\Delta\theta$ between the centers of two D-clusters. Panels (a)–(c) correspond to parameter $A_0 = 0.1$, 0.3, and 0.7, respectively. (d): The position $\Delta\theta_{\rm m}$ at which the probability is maximal varying with A_0. The red line is the fitting curve. Here $N = 256$, $\beta = 0.10$, and $A = 0.995$.

4. Analysis

The above results can be analyzed with the assistance of the Ott–Antonsen ansatz.[14,16] Following the line in Refs. [12]–[14], we assume that there is a probability density function $f(x,\omega,\theta,t)$ characterizing the state of the system. This function satisfies the continuity equation[12–15]

$$\frac{\partial f}{\partial t} + \frac{\partial}{\partial\theta}(fv) = 0, \tag{6}$$

where

$$v = \omega + A_0\sin\theta - \int_{-\pi}^{\pi} G(x-x') \times \int_{-\pi}^{\pi} \sin(\theta-\theta'+\alpha) f(x',\theta',t)\,{\rm d}\theta'\,{\rm d}x' \tag{7}$$

with $\theta = \theta(x)$ and $\theta' = \theta(x')$. The complex order parameter can be formulated as

$$Z \equiv R{\rm e}^{{\rm i}\Theta} = \int_{-\pi}^{\pi} G(x-x') \int_{-\pi}^{\pi} {\rm e}^{{\rm i}\theta'} f(x',\theta',t)\,{\rm d}\theta'\,{\rm d}x'. \tag{8}$$

In terms of the complex order parameter Z, then equation (7) can be rewritten as

$$v = \omega + A_0\sin\theta + \frac{\rm i}{2}[Z^*{\rm e}^{{\rm i}(\theta+\alpha)} - Z{\rm e}^{-{\rm i}(\theta+\alpha)}], \tag{9}$$

where Z^* denotes the complex conjugate of Z. Following Ott and Antonsen,[17,18] we have

$$f(x,\omega,\theta,t) = \frac{1}{2\pi}\left\{1 + \sum_{n=1}^{\infty}[(a(x,t){\rm e}^{{\rm i}\theta})^n + {\rm c.c.}]\right\}, \tag{10}$$

where c.c. is the complex conjugate of the previous term. In this work, we assign all oscillators to have the same natural frequency ($\omega = 0$). By substituting Eqs. (9) and (10) into Eqs. (6) and (8), we obtain

$$\frac{\partial a(x,t)}{\partial t} = \frac{1}{2}[(Z^*{\rm e}^{{\rm i}\alpha} - A_0) - (Z{\rm e}^{-{\rm i}\alpha} - A_0)a^2], \tag{11}$$

$$Z = \int_{-\pi}^{\pi} G(x-x')a^*(x',t)\,{\rm d}x'. \tag{12}$$

By numerically simulating these two equations, we obtain the time evolutions of $R(x)$ and $\Theta(x)$. The results are presented in Fig. 5. Clearly the main features presented in Fig. 1 by numerical simulations of the original equations of motion, such as four clusters, the frozen pattern of R and Θ and the distribution of $\Theta(x)$, are reproduced in Fig. 5.

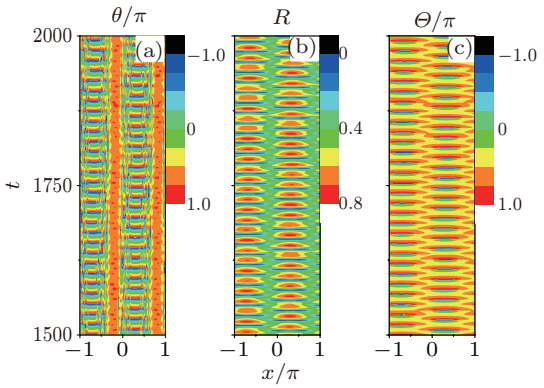


Fig. 5. (color online) Phase patterns for the four-cluster chimera state when the steady state is reached. Equations (11), (12), and (4) are integrated by using the Runge–Kutta method with fixed time step dt = 0.005, and the oscillator number $N = 256$. (a): The phase θ/π distribution of oscillators. (b) and (c): The modulus R and the phase Θ/π of the complex order parameter, respectively. $\beta = 0.1$, $A = 0.995$, and $A_0 = 0.4$.

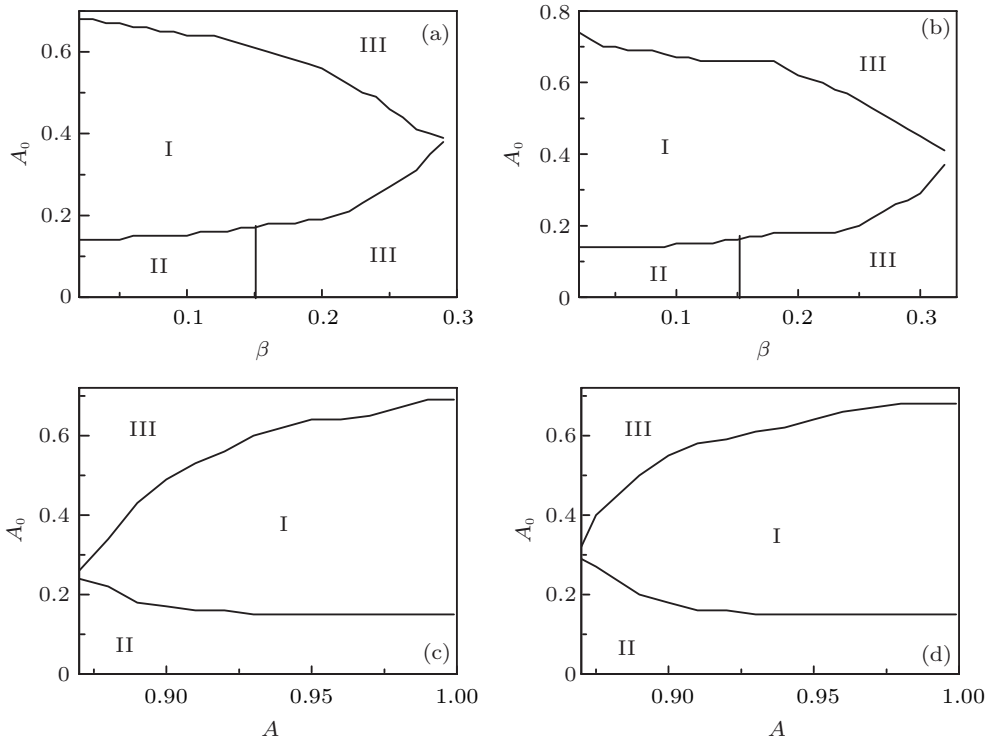


Fig. 6. Boundary of the four-cluster chimera state using the quasi-static process. (a) and (b): The phase diagram on the A_0–β plane for $A = 0.95$ and $A = 0.995$, respectively. (c) and (d): The phase diagram on the A_0–A for $\beta = 0.05$ and $\beta = 0.10$, respectively. The regions I, II, and III are parameter space of four-cluster chimera state, two-cluster chimera state, and completely synchronize state, respectively.

By using Eq. (1), we may probe the regime for the existence of the four-cluster chimera state in the parameter space depicted in Fig. 6. The parameter regions labelled with the symbols 'I', 'II', and 'III' corresponding to the regions of the four-cluster state, two-cluster chimera state, and complete synchronize state, respectively. From Figs. 6(a) and 6(b), one can see that the region of the four-cluster chimera state decreases with parameter β increasing. The four-cluster chimera state does not exist any longer if β is larger than the critical value β_c when the parameter A is fixed. The critical value β_c depends on parameter A. Beyond the stable regime for the four-cluster chimera state, the initial four-cluster chimera state may lose its stability. Above the upper boundary curves, the initial four-cluster chimera state evolves into the synchronized state. Below the lower boundary, the initial four-cluster chimera state tends to become a two-cluster chimera state if $\beta < 0.15$ and become the synchronized state if $\beta > 0.15$. From Figs. 6(c) and 6(d), it can be learned that A must exceed a critical value around $A = 0.87$ when the parameter β is fixed. This means that the effect of nonlocal coupling becomes stronger, and the region of the four-cluster chimera state is larger.

5. Conclusions

In this paper we studied the spatiotemporal dynamics of a 1D system consisting of non-locally coupled phase oscillators in the presence of an external potential. It is found that the system can evolve into a synchronized state, single-cluster chimera and two-cluster chimera states when the potential field is weak. As the external potential strength A_0 is increased to a critical value, a four-cluster chimera state emerges. Different from the clustered chimera states that have been studied previously, the oscillators of the synchronized clusters do not possess the same average frequency. For the four-cluster chimera state, we find that even if oscillators in different D-clusters have different instantaneous frequencies, they still evolve with the same average frequency. The phenomena induced phase difference between the oscillators in different D-clusters does not keep π, and the distribution of the phase difference has two peaks. If the A_0 is large enough, the system will step into a synchronization state. The numerical results are confirmed by the theoretical analysis based on the Ott–Antonsen ansatz.

Chimera may be a paradigm in studies of the unihemispheric sleep in neurology, which reveals the fact that many creatures sleep with only half of their brain while the other half is still active during the sleeping process.[19] By analyzing the recorded brain waves, it is found that the awake side of the brain shows a desynchronized electrical activity, corresponding to millions of neurons oscillating out of phase, whereas the sleeping side is highly synchronized. Nevertheless, the actions of the brain are highly complicated and the brain can deal with many tasks at the same time. This can be dynamically understood as the existence of many different synchronized clusters in the neurons network of brain. We expect the

studies of the four-cluster chimera state presented in this paper may shed some light on the investigations of the behaviors in neural networks.[20]

References

[1] Kuramoto Y and Battogtkh D 2002 *Nonlinear Phenomena in Complex Systems* **5** 380
[2] Tanaka D and Kuramoto Y 2003 *Phys. Rev. E* **68** 026219
[3] Abrams D M and Strogatz S H 2004 *Phys. Rev. Lett.* **93** 174102
[4] Kawamura Y 2007 *Phys. Rev. E* **75** 056204
[5] Omel'chenko O E, Maistrenko Y L and Tass P A 2008 *Phys. Rev. Lett.* **100** 044105
[6] Motter A E 2010 *Nat. Phys.* **6** 164
[7] Shima S I and Kuramoto Y 2004 *Phys. Rev. E* **69** 036213
[8] Martens E A, Laing C R and Strogatz S H 2010 *Phys. Rev. Lett.* **104** 044101
[9] Sheeba J H, Chandrasekar V K and Lakshmanan M 2010 *Phys. Rev. E* **81** 046203
[10] Sethia G C, Sen A and Atay F M 2008 *Phys. Rev. Lett.* **100** 144102
[11] Zhu Y, Li Y T, Zhang M and Yang J Z 2012 *Europhys. Lett.* **97** 10009
[12] Abrams D M, Mirollo R, Strogatz S H and Wiley D A 2008 *Phys. Rev. Lett.* **101** 084103
[13] Pikovsky A and Rosenblum M 2008 *Phys. Rev. Lett.* **101** 264103
[14] Laing C R 2009 *Physica D* **238** 1569
[15] Laing C R 2009 *Chaos* **19** 013113
[16] Ott E and Antonsen T M 2009 *Chaos* **18** 037113
[17] Ma R B, Wang J X and Liu Z H 2010 *Europhys. Lett.* **91** 40006
[18] Omel'chenko O E, Wolfrum M and Maistrenko Y L 2010 *Phys. Rev. E* **81** 065201
[19] Mathews C G, Lesku J A, Lima S L and Amlaner C J 2006 *Ethology* **112** 286
[20] Olmi S, Politi A and Torcini A 2010 *Europhys. Lett.* **92** 6007